International Journal of Scientific Research in Science and Technology
Print ISSN: 2395-6011 | Online ISSN: 2395-602X (www.ijsrst.com)
doi : https://doi.org/10.32628/IJSRST229367

Environmental Magnetism, Geochemical and Textural Characteristics of the Sediments of Beypore Estuary, Northern Kerala, India: Implication on Environmental Processes

B.S. Praseetha*[1,2], V.I. Tiju[1], T.N. Prakash[1,3], G. Sreenivasulu[4], R. Nagendra[5]

[1]Marine Geoscience Group, National Centre for Earth Science Studies, Thiruvananthapuram, Kerala, India
[2]Department of Marine Geology and Geophysics, Cochin University of Science and Technology, Cochin, Kerala, India
[3]National Institute of Advanced Studies, IISC Bangalore, Karnataka, India
[4]Sri Venkateshwara University, Tirupati, Andhra Pradesh, India
[5]Formerly, Department of Geology, Anna University, Chennai, Tamil Nadu, India
*Corresponding author: praseethabs@gmail.com

Article Info
Volume 9, Issue 3
Page Number : 314-334
Publication Issue
May-June-2022
Article History
Accepted : 10 May 2022
Published : 30 May 2022

ABSTRACT

The inter-relationship between the environmental magnetic parameters, geochemical and granulometric distribution are addressed in this paper to assess the environmental conditions employing the surficial sediments of Beypore Estuary, Kerala. The magnetic results elucidate the dominance of magnetic grain size in the lower estuary, magnetic concentration in the middle, and magnetic mineral in the upper estuary, respectively. The magnetic parameters confirm the presence of ferrimagnetic minerals such as magnetite in the estuary. The geochemical elements affinity attribute towards the lower estuary. Further, intense weathering in the lower estuary and moderate to weak weathering in the middle and upper estuary are observed which is reflected in the micro-texture features of quartz grains. The Beypore sediments are moderately polluted based on the pollution indices. The finding elucidates the combination of natural and anthropogenic activities, controlling the environmental conditions in the estuary.

Keywords : Estuary, Environmental magnetism, Geochemistry, Sediment texture

I. INTRODUCTION

An estuary is a dynamic system that connects the river and the ocean. The sedimentary archives are preserved, and several more sediment proxies aid in defining the depositional environment. The estuary is divided into three sections: the marine or lower estuary (free connection to the open sea), the middle estuary (mixing of saline and freshwater), and the upper estuary (upper or fluvial estuary) [1]. They are the natural sinks for heavy metals and magnetic minerals from a variety of sources, including natural and anthropogenic activities. Magnetic particles in coastal sediments are frequently produced from terrestrial

sources and transported by rivers and winds [2]. For the investigation of the source of pollution and identifying the method of transfer from source to sink, the link between magnetic susceptibility and heavy metal concentrations in marine, estuarine, and river sediments is well-established globally [3][4][5]. For a long time, the mode of transport, deposition, and diagenetic processes of magnetic minerals are influenced by environmental changes caused by climate deviations [6] [7]. Environmental magnetism (EM) has been shown to be a diagnostic tool in determining sediment provenance [8], post-depositional diagenetic changes [5], their source of pollution [10], [11a, b] [12] [13] [14], and paleo-monsoon variability [15] [16][17]. The magnetic characteristics of sediments are determined by the source-area composition [18], climatic circumstances, length and energy of the type, quantity, and particle size of magnetic minerals [19]. Sediment origin, hydrodynamic circumstances during transport, and the sedimentary environment will all influence these parameters. The steady state of geochemical distribution along the estuary is maintained in part by geochemical processes inside the estuarine sediment. [20] proposed a systematic investigation of magnetic characteristics of sediments for the central Kerala coast based on the Bharathapuzha River bed sediments to correlate the influence of both natural and human activities. The paper infers that higher concentrations of the pollution load index and combinations of magnetite and hematite have been related to extensive anthropogenic activities in the central Kerala region. Beypore, in northern Kerala, is noted for boat construction (named Uru), fishing, and timber business, as well as factories such as Gwalior Rayon, tile manufacture, and so on. Mud banks in the nearshore region of Beypore are very well-known. In the Beypore Estuary, numerous studies have been published, including those on saline intrusion [21], hydrography [22], monthly trends of residual salt and water fluxes, and transportation of suspended sediments [23], textural parameters and total organic carbon content [24], and suspended sediment distribution and mixing of water [25] and study on foraminifera [26]. However, because the environmental magnetic analysis of the Beypore sediments has a gap in research records, the integration of environmental magnetic, sedimentology and geochemical issues is considered with the ensuing objectives: (i) to determine the magnetic behavior of sediments in the environment and their pattern of dispersion, (ii) evaluating geochemical features in order to better understand the processes, transport pathways, weathering, and pollution aspects in the estuary; and (iii) decoding the environmental processes impacting the sediments using magnetic, geochemical, and textural affinity.

A. Beypore Estuary

The Beypore Estuary is the fourth largest estuary in Kerala (Fig.1a), the major riverine input to the estuary is the Chaliyar River (length of 169 km). Beypore is the point where the estuary meets the Arabian Sea and mangrove swamps stretch along the estuary's borders. The Chaliyar River (total drainage area of 2923 km^2) flows through Nilambur, Edavanna, Areekode, Vazhakad, Mavoor, Aakode, Feroke, and Beypore areas [27]. Many rivers, including the Chaliyarpuzha, Kallayipuzha, Korapuzha, and Poonoorpuzha, flow through the city, transporting sediments to the Arabian Sea. The harbours of Puthiyappa and Vellayil are located 8km north of the estuary. The average temperature in the basin ranges from 23.7°C to 30.9°C, with an average annual rainfall of 3000mm [28]. Some of the industries perceived in, around the estuary are textile, and sawmills, shipbreaking facilities, tile, and brick manufacturers. Physiographical, the territory is divided into three sections: sandy coastal plain, lateritic midland, and rocky highland. A sandy coastal strip and lateritic midland surround the region, which has an elevation of >1m MSL along the shore. Backwater with interconnecting canal networks receiving drainage from Kozhikode city characterizes the lowland area [29].

B. Geology of the area

The region's basement rock is composed of Archean

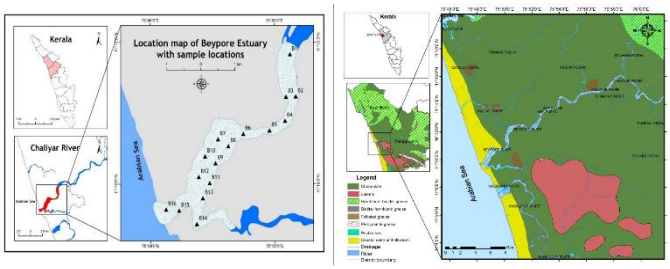

Figure 1. Study area map and the geological settings of the Beypore Estuary

charnockite and gneisses like biotite-hypersthene gneiss and biotite-hornblende-hypersthene gneiss [30]. Pebble beds are present on the banks of the Chaliyar River and the Beypore Estuary on rare occasions [31] [32]. Within the gneissic terrain to the north, east, and south of the Beypore, pockets of charnockite are recorded (Fig.1b) [27] [31] [33].

II. METHODS AND MATERIAL

In April 2015, the Van-Veen grab sampler was used to collect 16 surface sediment samples from the Beypore Estuary. The estuary is separated into three sections for ease of interpretation and discussion: upper estuary (B1-B5), middle estuary (B6-B12), and lower estuary (B13-B16). The fetched sediments were well-mixed for the magnetic, geochemical, and textural analyses. The low field magnetic susceptibility (χ), Frequency-dependent susceptibility (χ_{fd}), Anhysteretic Remanent Magnetization (χ_{ARM}), Isothermal Remanent Magnetization (IRM) of different field strength was analyzed following the standard procedure by employing the Barrington Susceptibility Meter (Model MS2B), Molspin AF demagnetizer and Magnetometer at the Environmental Magnetism Laboratory, Mangalore University [16] [34] [35] [36]. The sediment raw samples (wet) were packed into 8cm^3 non-magnetic plastic bottles, which were tightly packed using polyethylene covers. Barrington Susceptibility meter with a dual-frequency sensor was utilized to measure magnetic susceptibility at low (χlf: 0.47 kHz) and high (χhf: 4.7 kHz) frequencies. The sensor was calibrated by using the standard Fe_3O_4 (1%) solution. The frequency-dependent susceptibility (χfd %) was calculated from the low- and high-frequency susceptibility [34]. A Molspin AF demagnetizer (with an ARM attachment) was used to induce an anhysteretic remanent magnetization (ARM) in the samples, set with a peak alternating field of 100 mT and a DC biasing field of 0.04 mT. A Molspin spinner fluxgate magnetometer was used to measure the ARM. The susceptibility of ARM (χARM) was obtained by dividing the mass-specific ARM by the size of the biasing field [36]. Isothermal remnant magnetization (IRM) was induced in the samples at different field strengths (20, 60, 100, 300, 500, 600, and 1000 mT) using a Molspin pulse magnetizer. 1000mT was the maximum field, attainable in the environmental magnetism at the laboratory and was considered as the saturation isothermal remanent magnetization (SIRM). Inter-parametric ratio; S-ratio, χARM/χlf, χARM/SIRM, and SIRM/χlf were calculated to determine the magnetic mineralogy and grain size (Walden 1999b). The magnetic parameters and inter-parametric ratios investigated, as well as their units and interpretations [7] [9] [37].

The major oxides viz., SiO_2, Al_2O_3, MgO, MnO, Fe_2O_3, K_2O, Na_2O, TiO_2, and P_2O_5 were determined by using a sequential wavelength dispersive X-ray spectrometer (XRF Bruker model S4 Pioneer installed at XRF Laboratory, NCESS, Thiruvananthapuram). The LOI samples were converted into pellets under a hydraulic press at 20 Ton. The pressed pellets were subjected to XRF analysis based on the standard procedures (see the details, www.ncess-xrf.gov.in). The trace elements of the sediments were analysed by ICP-MS (Thermo-X series 2) at the Geosciences Division, Physical Research Laboratory (PRL), Ahmedabad. ~0.3g of the dried and powdered samples were exposed to closed digestion by treating with an acid mixture (HNO_3, HCl, and HF) in a microwave digestion system (Milestone, Start D). The

accuracy and precision of the results were monitored by repeat measurements of reference sediment standards (marine sediment standards MAG-1 and NOVA) and were recorded to be better than ±6 and ±4%, respectively [38]. The Rare Earth Element (REE) were analysed using ICP-MS (Perkin Elmer SCIEX Model 6100 ELAN DRCII at the National Geophysical Research Institute, Hyderabad, India). The powdered samples were analyzed based on the standard procedures and reference materials therein (MESS-3 and PAAS) [39].

The textural analysis of the samples was carried out following the method of [40]. The sediments were pre-treated with 30% H_2O_2 and 1N HCl to remove the organic matter and $CaCO_3$ contents. The representative of the treated samples was subjected to pipette analysis based on Stoke's law [41]. The pipetted and the sand fractions were processed based on the Gradistat software programme [42] for the computation of sand-silt-clay percentages and statistical parameters. The clay fraction (< 2μm) obtained from the pipette analysis is mounted on a grounded glass slide followed by the smearing technique [43]. The clay slide is then scanned (5°to 40° at 2°2θ/minute) using the PANalyticalX'pert PRO XRD facility at NCESS for the identification of clay-sized minerals and was confirmed by standard references [44] [45].

The surface micro-textures of quartz grains derived from the estuarine environment have been examined using a Scanning Electron Microscope (SEM) technique (SEM-EDS, TESCAN VEGA 3 LMU, SEM Laboratory, NCESS). The observed micro-texture features obtained from the SEM analysis were confirmed based on the standard references [46] [47]. The calcium carbonate and organic carbon contents were analysed by the titration methods [48]. The spatial distribution of heavy metal and magnetic parameters were plotted by interpolation methods through an IDW algorithm (Arc GIS 10.3). The multivariate statistical analyses; correlation matrixes, cluster analyses, and Principal Component Analysis (PCA) were performed by using SPSS software.

To assess the present pollution status of the estuary, the Geoaccumulation Index (Igeo), Enrichment Factor (EF), Contamination Factor (CF), and Pollution Load Index (PLI) were applied. According to [49], Igeo was calculated as follows;

$$Igeo=\log_2 [Cn/1.5*Bn]$$

Where Cn is the estimated value of the analytical metal n in the sediments, Bn is the background value of the continental crust averages [50].

Enrichment Factor (EF) measures the extent of anthropogenic influence on the sediments [51]. In this study, Fe is used for the normalizing elements [52]. The geochemical background values are followed with the reference of [50].
According to [53]

$$EF = \frac{\text{Trace element concentration in } \frac{\text{sample}}{\text{Fe}} \text{ content in the sample}}{\text{Trace metal content in the } \frac{\text{UCC}}{\text{Fe}} \text{ content in the UCC}}$$

Contamination Factor (CF) is calculated by using the formula

$$CF=C_{metal}/C_{background\ value}$$

Where C_{metal} is the total metal content, and $C_{background}$ represents the background value of the sediments [50].
PLI was calculated using the following equation [54]

PL1= (CF1*CF2*CF3*CF4*……*CFn) 1/n

Where n is the number of elements and CF represents the contamination factor.

III. RESULTS AND DISCUSSION

The magnetic mineral variability, elemental concentration, textural characteristics, and their implications for the environmental processes for the Beypore Estuary sediment are discussed.

A. Magnetic concentration, grain size, and mineralogy of the sediments

The magnetic susceptibility (χlf) is a concentration-dependent parameter viz., signals from the ferrimagnetic and canted antiferromagnetic minerals. χlf may also be influenced by the presence of diamagnetic and paramagnetic minerals [7] and, the composition and grain size of the magnetic minerals [11] [12]. χlf of sediments shows fluctuation ranging from $15.84*10^{-8}$ m^3/kg to $135.43*10^{-8}$ m^3/kg with an average of $58.08*10^{8}$ m^3/kg. The maximum value of χlf is recorded in B6 and B8 stations with the least value in the bar-mouth (stations B15 and B16). The spatial distribution for the magnetic properties of sediments reveals a dissimilarity in their pattern (Fig.2 A to G).

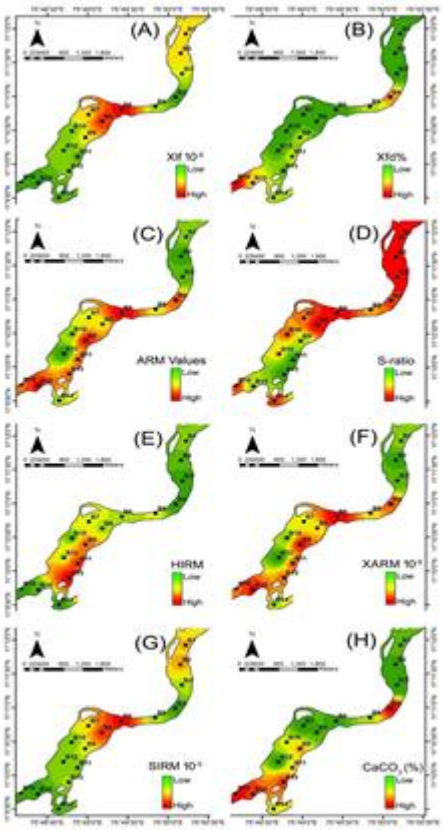

Figure 2. Spatial variation of magnetic parameters for the samples along the estuary

The χfd%, ARM, HIRM, and χARM distributions display low values whereas, χlf and SIRM show moderate values, and only S-ratio shows a higher value in the upper estuary. The middle estuary shows a critical high variation in the magnetic parameters viz., χlf, ARM, S-ratio indicates the anthropogenic activities and the course of the water flow in the form of meandering loops in the middle estuary. In the lower estuary, the magnetic parameters such as SIRM, HIRM, and χlf display lower values whereas, χfd%, ARM, S-ratio, and χARM exhibit a higher concentration indicating coarse grain size parameters. This may be related to the hydrodynamic activities like the winnowing action of the sediments being dominant as well as the dredging activities more dynamic in this region. The S-ratio gives the relative proportions of ferrimagnetic and anti-ferromagnetic minerals (a high ratio means = a relatively high proportion of ferrimagnets). The S-ratios vary between 0.894 and 0.981, indicating the presence of ferrimagnetic minerals (value corresponds close to 1 to the predominance of ferrimagnetic minerals, Fig.2D). The values of χARM and SIRM vary from 0.109 to $0.291*10^{-5}$ m^3/kg and 122.24 to $687.55*10^{-5}$ Am^2/kg (Table 1) with low values towards the bar-mouth (lower estuary). The observed results from these parameters (χlf, χARM, SIRM) indicate the presence of ferrimagnetic minerals such as magnetite in the estuary [17]. The χARM/SIRM ratio ranges from $33.73 \times 10^{-5} mA^{-1}$ to 186×10^{-5} m A^{-1} ; moderately low for upper and middle estuary compared to higher in the lower estuary. The magnetic grain size distribution was determined using the χARM/SIRM vs. χfd% biplot (Fig. 3) [34].

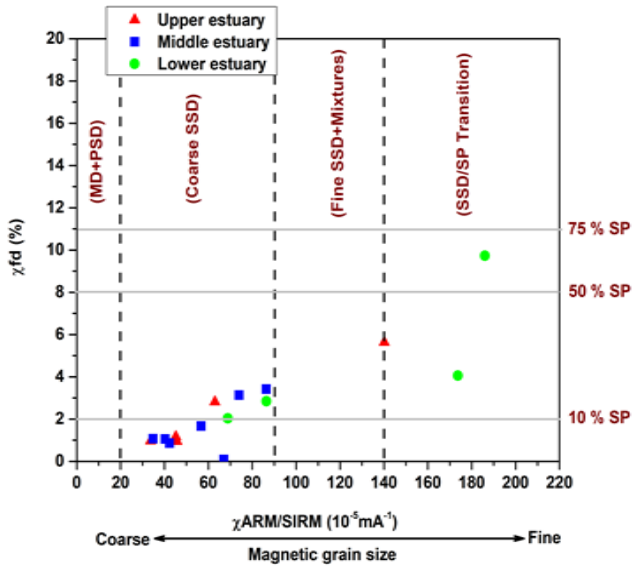

Figure 3. Bivariate plot of χARM/SIRM vs. χfd% reveals that the sediment samples falls in the coarse SSD region with <50% SP grains and <8 χfd%

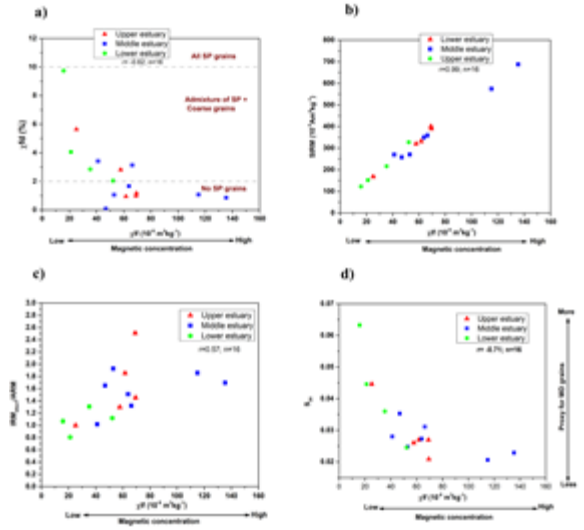

Figure 4. Scatter plots of (a) χlf vs χfd% reveals the presence of SP and coarser non-SP grains (b) χlf vs SIRM suggesting that the magnetic signal of the surface sediments are dominated by magnetically strong ferrimagnetic minerals (c) χlf vs IRM20mT/SIRM plot corroborates the results of magnetic grain sizes and (d) χlf vs S20 reflects lesser proportions of MD grains

The plot reveals that the sediment samples falls in the coarse SSD region with <50% SP grains and <8 χfd%, respectively. Fine grain size of magnetic minerals is indicated by larger values of the χARM/SIRM and coarser magnetic grains by smaller values [55]. Frequency-dependent susceptibility (χfd) is an indicator of the proportion of ultrafine superparamagnetic (SP) grains [56]. The χfd values in this study ranged from 0.08 to 9.73% (Table 1). The χfd% (0.09 to 9.73) reflects the presence of multi-domain and stable single domain size [7]. High χfd% values suggest significant concentrations of superparamagnetic grains in the sediments [56], whereas low χfd% values < 2%indicate the absence of SP grains [34] (Table 1). The bivariate plot of the percentage of frequency-dependent (χfd %) versus χlf reveals the presence of SP and coarser non-SP grains (Fig.4a). The scatter plot (Fig. 4a) between χlf and χfd%) exhibit that majority of the estuary samples possess χfd% values < 10% and fall in the region of "Admixture of SP + coarse grain to no SP grains" suggesting contribution from SP grains to the magnetic properties of the Beypore surface sediments [57]. Negative correlation is evident between χlf and χfd % (Fig. 4a), and a statistically strong positive relationship is evident between χlf and SIRM (r = 0.99, n = 25; Fig. 4b) suggesting that the magnetic signal of the surface sediments from Beypore is dominated by magnetically strong ferrimagnetic minerals. The χlf vs IRM_{20mT}/SIRM plot corroborates the results of magnetic grain sizes (Fig. 4c). The S_{20} ($IRM_{20\ mT}$/ARM) indicate a mixed assemblage of coarse SSD and MD grains [57]. The lower S_{20} values in this study reflects lesser proportions of MD grains and $IRM_{20\ mT}$/ARM values <10 indicate significant contributions from SSD grains (Fig.4d) [55]. This also confirms with negative correlation of the parameter.

The IRM reading v/s different field strengths (20, 60, 100, 300, 500, 600, and 1000 mT) indicates that estuarine sediments are saturated at the field below 300 mT depicting the presence of a high magnetic concentration of ferrimagnetic mineral; magnetite or Ti-magnetite (Fig.5).

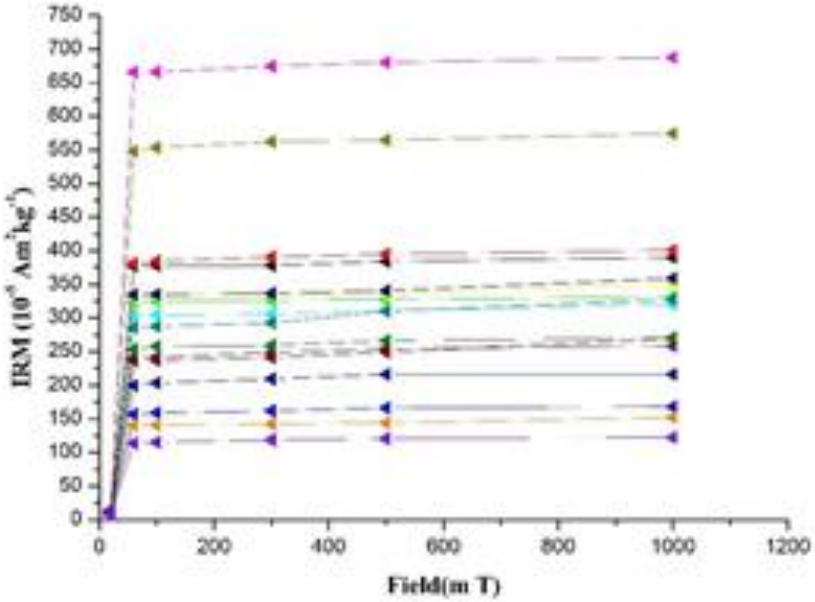

Figure 5. Isothermal remanent magnetization (IRM) acquisition curves for surficial sediment samples of Beypore Estuary

Table 1. Statistics of the mineral magnetic parameters of the Beypore Estuarine sediments

	χ (10^{-8} m^3kg^{-1})	χfd (10^{-8} m^3kg^{-1})	χfd (%)	SIRM (10^{-5} Am^2kg^{-1})	SIRM/ χlf (10^3 Am^{-1})	χ ARM/ χlf	χARM/SIRM ($10^{-5}mA^{-1}$)	S-ratio	ARM	Sand (%)	Silt (%)	Clay (%)
N	16	16	16	16	16	16	16	16	16	16	16	16
Min	15.84	0.04	0.09	122.24	4.99	0.0017	0.0003	0.90	3.47	4.81	0.37	5.06
Max	135.43	2.08	9.73	687.55	7.72	0.009	0.0018	0.98	9.26	93.11	27.89	72.69
Mean	58.09	1.07	2.59	324.89	5.90	0.0049	0.0008	0.96	6.52	63.61	7.52	28.23
Standard deviation	30.42	142.18	142.18	142.18	0.76	0.0037	0.0005	0.03	1.52	33.16	7.99	25.52
Kurtosis	1.56	1.56	1.56	1.56	0.38	1.7953	1.0417	1.47	-0.32	-1.21	1.46	-1.19
Skewness	1.08	1.08	1.08	1.08	1.03	1.6428	1.4252	-1.45	-0.17	-0.79	1.53	0.80

The condition of χARM/χ <40 and χARM/χfd <1000 indicate the absence of bacterial magnetite. The concentration parameters (χlf, χARM, SIRM) is more dominant in the middle whereas the grain size of magnetic particles is dominant in the lower estuary. The mineralogy shows mixed variety. In the lower estuary, magnetic grain size doesn't have any control over textural grain size

B. Geochemical appraisal- spatial distribution, paleo-weathering, and anthropogenic activities

The average concentration of SiO_2, MnO, and Na_2O are enriched in the upper estuary (avg: 72.53, 0.034, 1.24, respectively) whereas other elements (TiO_2, Al_2O_3, Fe_2O_3, CaO, MgO, K_2O, P_2O_5) are depleted. In the lower estuary, the average value of Al_2O_3 (14.73%) and TiO_2 (0.65%) is enriched with depletion of SiO_2 indicating the fineness of grain size linked to fractionation processes. The trace elements, attribute higher concentration in the lower estuary as compared to the middle and upper estuary. The average concentrations of Cr (169 ppm), Ni (49.26 ppm), Zn

(50.16 ppm), and Pb (10.32 ppm) are enriched in the lower estuary except for Cu (35.86 ppm). Generally, the concentration of Ni, Cu, Zn, Cr, and Pb varies from 13.4-82.3 ppm, 10.8-80.4 ppm, 17.2-107 ppm, 71-240 ppm, and 4.1-168 ppm, individually along the estuary. At the B4 station, the Cr and Cu concentration are higher than in the adjacent station as it could be due to the terrigenous influx of domestic waste. Moreover, the B4 station is located in the meandering loop of the Chaliyar River below the Feroke railway bridge. The spatial distribution (Fig. 6) reveals that in the middle estuary (B6 station), there is a depletion in the Cr and Cu concentrations with no change in Zn and Pb contents. In the lower estuary (particularly B12 and B13 stations), the Cr and Ni contents are reduced with minor variation in Cu, Zn, and Pb concentration where the smaller tributaries adjoined to the main channel leading to the accumulation of heavy metals.

The higher concentration of Cu in the upper estuary may be related to industrial activities. The high enrichment of Al, Fe, Cr, and Ni contents in the upper estuary may be attributed to the entrapment of these metals in the fine-grained sediments which were derived from the fluvial inputs.

The plot for the normalization of major and trace elements against Upper Continental Crust (UCC) [58] [59] is illustrated in figure 7. In the lower estuary, the oxides viz., TiO_2, MgO, Fe_2O_3, and K_2O show enrichment whereas depletion of Al_2O_3, MnO, CaO, Na_2O, and K_2O are observed as compared to UCC values. The middle and upper estuary show similar trends of depletion for Fe_2O_3, MgO, Na_2O, K_2O except for SiO_2 and TiO_2 contents. While in the case of trace elements (Fig. 7b), Cr and Ni have a high concentration in all three sections (upper, middle, and lower) of the estuary. The trace elements such as Cr, Ni, Cu, Ga, Rb, Sr, Ba, La, and Ce show similar trends in the upper and middle estuary except for Zn content.

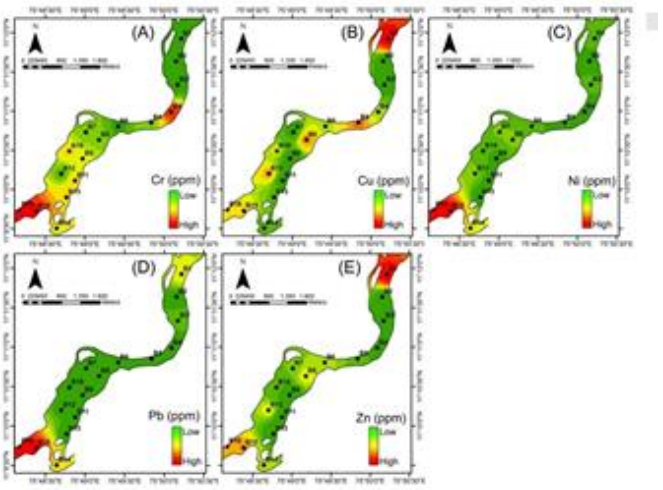

Figure 6. Spatial distribution of heavy metal assemblages in Beypore Estuary sediments

The higher concentration of Cr, Cu, in the estuarine sediments could be the residual of earlier deposited polluted effluents from the surrounding factories. During the pre-monsoon, the pollution load in the estuary will be difficult to flush out, since the buoyancy of the incoming freshwater is inadequate to overcome the mixing caused by strong tidal currents at the bar-mouth and estuary area [60].

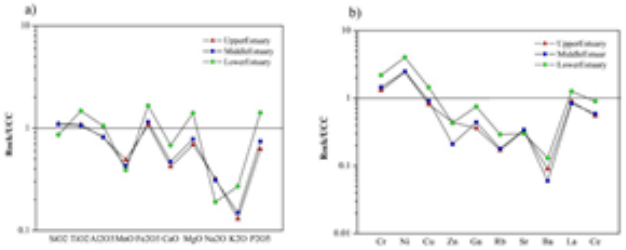

Figure 7. The normalization of major &trace elements against Upper Continental Crust UCC: [58] [59]

The REE elements (La, Ce, Pr, Nd, Sm, Eu, Tb, Dy, Ho, Er, Tm, Yb, Lu) were analyzed to define the concentration and trend of estuarine sediments. The concentration of total REE is high in the lower estuary (119.31 ppm) than in the upper (70.33 ppm) and middle (58.18 ppm) estuary. The dominance of LREE is more pronounced as compared to HREE in the estuarine sediments. The concentration of LREE exhibit two-fold enrichment in the lower estuary (106.64 ppm) as

compared to the middle (62.37 ppm) and upper (51.88 ppm) estuary. The calculated Ce anomaly in the study area ranges from -0.022 to 0.039 ppm. A positive Ce anomaly occurs, when Ce is enhanced relative to its adjoining elements and might have resulted from the existence of Fe–Mn oxyhydroxides [61] [62]. A negative Ce-anomaly represents the presence of siliceous organisms and Bementite [62]. The positive Ce-anomaly could be resulted due to the oxidation of Ce^{3+} to Ce^{4+} and assimilation into Mn oxyhydroxide phases as CeO_2. It is observed that Ce-anomaly in the tropical rivers and estuaries is mainly due to the leaching of Ce in oxides, especially iron oxyhydroxides [63]. Most of the station in the study area shows a positive Ce anomaly depicting the predominance of an oxic environment.

Eu anomaly is expressed as Eu/Eu* where Eu is the concentration of Eu in the sediments normalized with shale value and Eu* is a predicted value obtained by linear interpolation of Sm/Sm* and Gd/Gd*. The Eu anomaly in the Beypore sediments ranges from 0.76 to 2.54 indicating a significant positive anomaly relating to the origin of REEs from the alkali-feldspars [58]. Processes of seawater dilution and acid neutralization cause significant effects upon REE fractionation between the aqueous solution and sediments. This study described [64] the results of a recent investigation into such processes in the sediments of the Tinto and Odiel estuary.

The Chemical Index of Alteration (CIA) is used to quantify the degree of weathering intensity of clastic sediments and sedimentary rocks [65]. CIA measures the degree of alteration of feldspar to clay minerals, during weathering; accordingly leaching of Ca, Na and K through soil solution subsequently increases the relative abundance of Al content in the sediments resulting in the enrichment of CIA values [65]. The CIA value is calculated using the molecular proportions [65] as shown in the equation below:

$CIA= [Al_2O_3/ (Al_2O_3+CaO^*+Na_2O+K_2O)] \times 100$,

Where, CaO* is the amount of CaO assimilated in the silicate fraction of the rock (correction for CaO from carbonate contribution was not computed due to the absence of CO_2 value).

Thus, to calculate CaO* from the silicate fraction, the hypothesis proposed by [66] is assumed. In this regard, CaO values were accepted if $CaO < Na_2O$; subsequently, when $CaO > Na_2O$, it was presumed that the concentration of CaO equals that of Na_2O. The CIA values for the upper, middle, and lower estuary ranges from 73.51-84.6 (avg. 77.46); 72.14-81.77(avg. 77.47); 73.14-80.99 (avg. 77.25) respectively indicating the moderate weathering. The variation in the weathering intensity of the study area advocates that physical sorting of sediments during transportation and deposition leads to the enrichment of quartz and feldspar with heavy minerals in the coarse fraction and weathered minerals in the suspended load sediments [67].

To distinguish the source rock composition, diagenetic effects, and tectonism in the source area, the A-CN-K diagram was plotted using the molar ratios of Al_2O_3 (aluminous clays), $CaO + Na_2O$ (plagioclase), and K_2O (K-feldspar) [68] (Fig. 8a). Generally, the Beypore sediments are clustered differently indicating low-moderate-high weathering intensity. Moreover, most of the samples fall on the line of A-CN line which indicates the source is maybe from the plagioclase domain. The plot reveals that the upper estuary falls along the marginal line of weak and intermediate weathering except for one sample falling in the intermediate and strong weathering. The middle estuary and the lower estuary depict intermediate and strong weathering. The Index of compositional variability (ICV) is applied to evaluate the original detrital mineralogy and is calculated using the formula $ICV = [(Fe_2O_3 + K_2O + Na_2O + CaO + MgO + TiO_2)/Al_2O_3]$ [69]. The upper, middle and lower estuary sediments have ICV values ranging from 0.77 to 0.92, 0.8 to 1.1, and 0.84 to 1.11, respectively. The ICV and CIA values were plotted in order to understand the weathering and sediment maturity [70]. The plot reveals that most of the upper estuary sediments fall in the marginal line of immature and mature weak weathering as compared

to PAAS value (0.85) (Fig. 8b). The sediments of the middle estuary show a mixing of weak and intense weathering along the margin line of immature and mature conditions whereas the lower estuary shows immaturity under intense weathering.

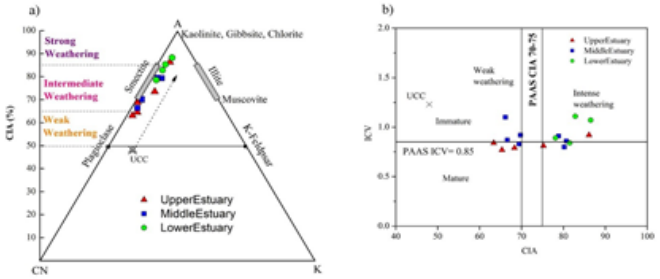

Figure 8. (a) A-CN-K (Al_2O_3-CaO*+Na_2O-K_2O, in molecular proportion) general weathering trend and intensity of weathering in the source region is shown in the ternary diagram(after [65]), (b) ICV vs CIA plot shows the maturity and intensity of chemical weathering for the sediment (after [70])

This confirms that the estuarine sediments are geochemically immature and derived from weak to moderately weathered sources with rich in rock-forming detrital minerals than clay minerals [69]. The SiO_2/Al_2O_3 ratio varies from 2.94 to 8.23 (upper estuary), 4.42 to 7.00 (middle estuary), and 2.64-7.99 in the lower estuary showing more than the PAAS value (SiO_2/Al_2O_3 ~ 3.3), indicating high textural maturity. The sediment source rocks can be identified based on the Al_2O_3/TiO_2 ratios to identify these elements associated with felsic and mafic minerals, respectively [71]. The Al_2O_3/TiO_2 ratio ranging from 3 to 8, 8-12, and 21-70 demarcate mafic, intermediate, and felsic igneous source rocks. The result of the Al_2O_3/TiO_2 ratio of sediments exhibits values ranging from 21.25 to 27.47 for the upper, 16.24 to 27 for the middle, and 18.98 to 34.1 for the lower estuary indicating a felsic igneous source. The K and Rb are used as an indicator for source composition that is sensitive to sedimentary recycling process [72]. In the K_2O vs. Rb (Fig. 9a) plot attributes the sediments of the lower estuary are acid+intermediate composition and the upper and middle estuary are basic in composition, this is because of enrichment of quartz and depletion of clay minerals. All the sediments are falling along the marginal line showing a uniform K/Rb ratio of 230. The high Rb concentrations (> 40 ppm) in the lower estuary elucidate the chemically coherent nature and are derived from rocks of intermediate and acidic compositions [73] [74]. In addition, a major oxide-based discriminant function diagram [75] is utilized to understand the provenance signature of the studied sediments from the estuary (Fig. 9b). The discriminant diagram depicts that the sediments from the upper estuary clustered in the domain of quartoze sedimentary provenance whereas the middle and the lower estuary clustered in the mafic igneous provenance which indicates that these quartzose sediments are derived from the recycled source of mature continental provenance [75]. Moreover, the sediment pattern along the upper estuary reveals the dominants of sand content enabling the SiO_2 content. Some of the lower and middle estuaries fall in the mafic igneous provenance, which shows the presence of more mafic minerals (i.e. pyroxenes and biotite) [76] TiO_2 vs. Ni diagram (after [72]) were plotted for the estuary sediments (Fig. 9c).

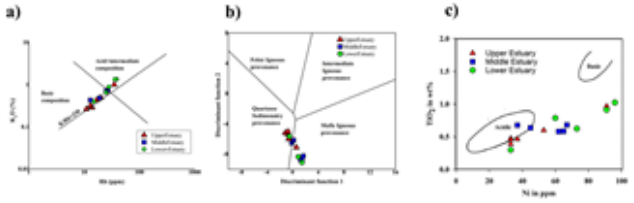

Figure 9. (a) K_2O *vs.* Rb plot shows the provenance field, representing coastal environments b) Discriminant function diagram of the core sediments from coastal plain, estuary and offshore depositional settings [75]. The discriminant functions are: Discriminant Function 1 = (-1.773×TiO_2) + (0.607×Al_2O_3) + (0.760×Fe_2O_3) + (-1.500×MgO) + (0.616×CaO) + (0.509×Na_2O) + (-1.224×K_2O) + (-9.090); Discriminant Function 2 = (0.445×TiO_2) + (0.070×Al_2O_3) + (-0.250×Fe_2O_3) + (-1.142 ×MgO) + (0.438×CaO) + (1.475×Na_2O) + (-

1.426×K_2O) + (-6.861). (c) TiO_2 *vs.* Ni diagram for the core sediments representing coastal environments of southern Kerala (after [72])

A few sediment samples from the upper and middle estuary falls clustered near the domain of acidic composition whereas the middle and lower estuary falls away from the acidic domain indicating the fractionation of sediments. Moreover, the higher Ni content is observed for the upper and middle estuary which indicates that Ni is more fractionated from the source rocks which are meagre in TiO_2-bearing minerals and thus comparable to intermediate to felsic source rocks. Also, Ni content in the estuarine sediments can be originated from the laterite and is related with the clay fraction of the sediments [76]. The sediments of lower estuary are composed of silty clay which corroborate the fractionation of Ni content. The pollution status of the estuary is studied with the determination of the Geoaccumulation Index (Igeo), Enrichment Factor (EF), Contamination Factor (CF) and Pollution Load Index (PLI). There are seven classes of sediment quality based on Igeo index, i.e., 0<uncontaminated; 0-1 uncontaminated to moderately contaminated; 1-2 moderately contaminated; 2-3 moderately to strongly contaminated; 3-4 strongly contaminated; 4-5 strongly to extremely contaminated; >5 extremely contaminated. The results reveals that the Cr and Cu are unpolluted to moderately contaminated category and other heavy metals are within the uncontaminated class (Fig. 10a).

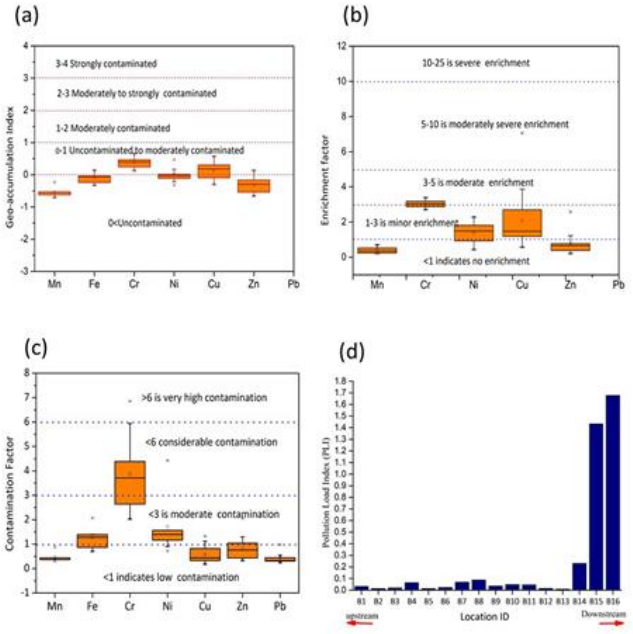

Figure 10. Box plots for (a) Geo-accumulation index, (b) Enrichment factor, (c) Contamination factor and (d) Pollution load index of the Beypore Estuary sediment.

The sources of these elements into the river and estuary are from tile factory, electroplating, metal manufacturing etc. similar observation were reported elsewhere [77]. The EF is applied to assess the extent of anthropogenic influence on the sediments. The Cr content in Beypore sediments exhibit moderate enrichment, the Ni and Cu are having minor enrichment (Fig. 10b).These contamination may be due to the domestic effluent discharges, small scale industries such as tile factory and dredging in the port areas [78]. The CF index is effectively used for the assessment of metal pollution. The CF values are categorized into four groups. <1 low contamination; <3 moderate contamination; <6 considerable contamination; and >6 very high contamination [79]. The result Cr shows considerable contamination, Ni and Fe is in moderate contamination, and other heavy metals indicate low contamination (Fig. 10c). Based on PLI values, the Beypore Estuary sediments are categorized under the non-polluted sediments, the station B15 and B16 of the confluence zone are placed under a polluted environment (PLI >1) (Fig. 10D).

C. Sedimentological and Mineralogical behavior of the sediments- grain size, transport and depositional environment.

The textural study (Table 2) shows that the sediments in the upper estuary are primarily sand (84.67 to 93.11%), with the exception of one station (B4; 12.48 percent) where the material is clayey sand. In the upper estuary, fine sediment is almost negligible. With low silt content and a rise in clay content, the middle estuary sand ranges from 74.31 to 93.09 percent (Fig. 11 and Table 2), showing a mixed variety of sediment types in the form of sand, clayey sand, and sandy clay, respectively.

The heavy mineral concentration is more prevalent in the middle estuary (range: 0.28 to 22.96 percent, avg.10.33 percent), followed by the upper (range: 3.35 to 13.57% avg.8.53%) and lower estuaries (range: 1.14 to 13.6%, avg.6.48 %). The presence of heavy minerals and the diversity in sediment distribution corroborate the deposition of heterogeneous (sand, clayey sand, and sandy clay) sediments in the investigated area. This could be attributed to energy fluctuations and sediment fractionation dependent on the hydrodynamic regime that exists in the estuary. The lower estuary (range: 1.28 to 18.08%, avg. 10.58%) has a higher calcium carbonate enrichment than the upper (range: 0.08 to 16.48%, avg. 6.2%) and middle estuaries (range: 2.08 to 10.28%, avg. 5.8%), respectively. The average TOC content in the upper and middle estuaries is minimal (avg. 0.28%; 0.41%, respectively), but the lower estuary shows considerable enrichment (avg. 3.31%).

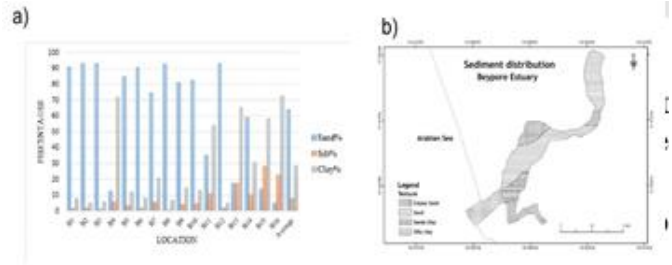

Figure 11. a) The variation of Sand-Silt-Clay percentages of the Beypore estuarine sediments. b) Sediment distribution of Beypore Estuary

Table 2. Textural parameters of Beypore estuarine sediments

Stations	Sand (%)	Silt (%)	Clay (%)	Mean M_z	Standard Deviation	Skewness S_k	Kurtosis K_g	Remarks			
B1(Upper)	90.67	1.63	7.7	1.466	2.129	0.45	4.3	MS	VPS	VFSk	ELKg
B2	92.91	2.03	5.06	1.629	1.581	0.253	2.834	MS	PS	FSk	VLKg
B3	93.11	1.18	5.71	1.504	1.75	0.325	3.397	MS	PS	VFSk	ELKg
B4	12.48	5.61	71.91	9.534	2.926	-0.733	1.091	C	VPS	VCSk	MKg
B5	84.67	3.13	12.19	2.135	2.636	0.598	3.292	FS	VPS	VFSk	ELKg
B6(Middle)	90.17	1.82	8.01	0.775	2.591	0.36	3.175	CS	VPS	VFSk	ELKg
B7	74.31	5.24	20.44	4.433	3.947	0.752	1.391	VCS	VPS	VFSk	LKg
B8	92.68	0.37	6.95	0.143	2.54	0.506	2.311	CS	VPS	VFSk	VLKg
B9	80.92	4.21	14.86	2.077	3.979	0.62	2.105	FS	VPS	VFSk	VLKg
B10	82.54	4.62	12.84	2.675	3.061	0.753	2.961	FS	VPS	VFSk	VLKg
B11	34.87	10.85	54.27	6.555	5.032	-0.535	0.491	MS	EPS	VCSk	VLKg
B12	93.09	1.83	5.07	0.249	2.192	0.171	1.861	CS	VPS	FSk	VLKg
B13(Lower)	17.51	17.28	65.2	8.492	3.903	-0.768	0.939	VFS	VPS	VCSk	MKg
B14	59.03	10.2	30.77	5.883	3.552	-0.086	0.938	CS	VPS	SYM	MKg VPKg
B15	14.04	27.89	58.07	8.541	3.123	-0.528	0.534	VFS	VPS	VCSk	

(MS-Medium Sand,C-Clay,FS-Fine Sand,CS-Coarse Sand, PS-Poorly Sorted, FSk-Fine skewed, SYM-Symmetrical, CSk-Coarse skewed, Kg- Platykurtic, MKg- Mesokurtic)

The heavy mineral concentration is more prevalent in the middle estuary (range: 0.28 to 22.96 percent, avg.10.33 percent), followed by the upper (range: 3.35 to 13.57% avg.8.53%) and lower estuaries (range: 1.14 to 13.6%, avg.6.48 %). The presence of heavy minerals and the diversity in sediment distribution corroborate the deposition of heterogeneous (sand, clayey sand, and sandy clay) sediments in the investigated area. This could be attributed to energy fluctuations and sediment fractionation dependent on the hydrodynamic regime that exists in the estuary. The lower estuary (range: 1.28 to 18.08%, avg. 10.58%) has a higher calcium carbonate enrichment than the upper (range: 0.08 to 16.48%, avg. 6.2%) and middle estuaries (range: 2.08 to 10.28%, avg. 5.8%), respectively. The average TOC content in the upper and middle estuaries is minimal (avg. 0.28%; 0.41%, respectively), but the lower estuary shows considerable enrichment (avg. 3.31%).

Climate, hydrography, geology, geography, and denudation processes are all factors in the creation of clay minerals [43]. The clay minerals in the sediment show that kaolinite is the most abundant, followed by illite, gibbsite, and Montmorillonite. The presence of Montmorillonite in the lower estuary may be seen in the down variation of the clay mineral (Fig. 12), whereas kaolinite and gibbsite have a well-crystalline peak in the region. It's possible that the occurrence of montmorillonite is attributable to the movement of

these minerals from the Deccan Trap [80]. The chemical weathering of the region's hinterland, including laterite, charnockite, and gneisses, is linked to the prevalence of kaolinite and gibbsite. The fluvial, aeolian, marine, and glacial environments and sedimentation processes are distinguished by the micro-texture of quartz grain [46] [81]. In the upper estuary, grains are angular and show dominant mechanical features such as conchoidal fracture, mechanical upturned plates, parallel steps, and fracture plates, breakage blocks plates, and abrasion (Fig. 13 A-C), whereas chemical features such as etch pits (Fig. 13 D) are negligible, indicating micro-textures of high mechanical features of crystalline rocks and grain to grain collision of river water sediments under high-energy conditions [82] [83] [84].

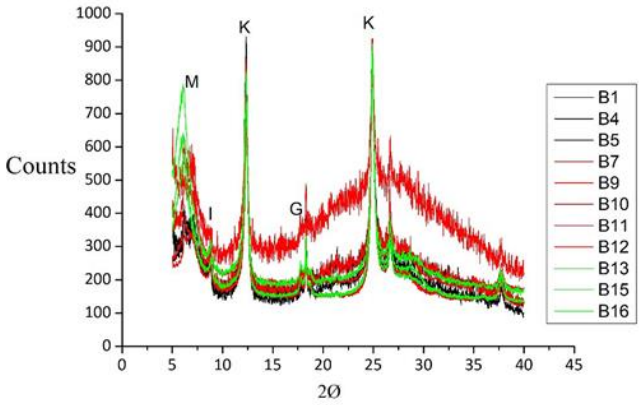

Figure 12. Distribution of clay minerals, Beypore Estuary (M-Montmorillonite, I-Illite, G-Gibbsite, K-Kaolinite)

In the middle estuary, the grains are sub-angular exhibiting the mechanical features such as conchoidal fracture, arcuate steps, and abrasion (Fig. 13 E, F) indicating mechanical processes. But these features are modified through silica solution in the form of silica plastering leading to the formation of chemical features like silica pellicle, chemical etching and traces of amorphous silica (Fig. 13. G, H). The results signifies the grains underwent mechanical and chemical alterations. The quartz grains of the lower estuary are sub-rounded (Fig. 13 I) indicating a substantial quantity of reworked sediments [81]. Here, the mechanical features such as conchoidal fracture, fracture plates and upturned plates are totally masked through the chemical solution leading to the formation of branching solution, silica crevasses, pressure solution, solution pits and dissolution etching (Fig. 13 J-L) indicating prolonged resident time leading to diagenesis [85].

Here, the mechanical features such as conchoidal fracture, fracture plates and upturned plates are totally masked through the chemical solution leading to the formation of branching solution, silica crevasses, pressure solution, solution pits and dissolution etching (Fig. 13 J-L) indicating prolonged resident time leading to diagenesis [85].

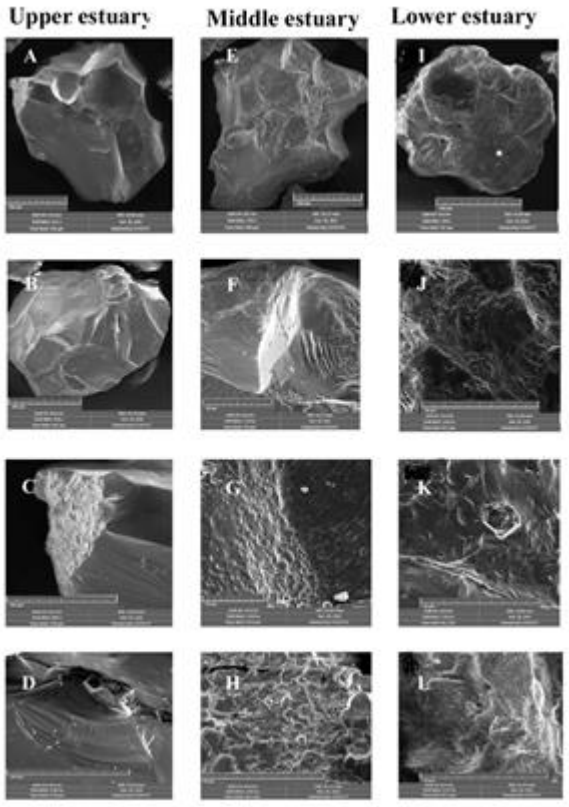

Figure 13. Quartz grains micro-textures of Upper estuary: A- Angular grains, B- Conchoidal fractures, C- Mechanical upturned plates, D- Parallel steps with amorphous silica; Middle estuary: E- Sub-angular, F- Arcuate steps, G- Silica pellicles, H- Chemical etching;

Lower estuary: I- Sub-rounded, J- Branching solution, K- Silica crevasses and L- Dissolution etching

The features further confirm that the grains were exposed to a high-energy chemical environment [46] under fluvio-marine conditions [84] [86].These results corroborate the sediment type of silty clay and the intermediate to strong weathering in the lower estuary.

D. Implication of environmental processes

To better understand the dynamic sedimentary environment, which can be reflected in sediment size, magnetic, heavy metals, and trace elements, Pearson's correlation analysis, factor analysis (PCA), and cluster analysis were employed using these variables. In this study, the χfd values suggest that the sediment contains an admixture of both SP and coarse magnetic grains. It exhibits a negative correlation with the χlf suggesting that the SP grains do not have any control on χlf values. The negative and positive correlation of χlf with geochemical elements (Cu, Cr, Zn, Ni, Pb) signifies the magnetic minerals are derived from terrigenous sources [87]. The ratios, χARM/SIRM and SIRM/ χlf show a negative correlation with χlf (r= -0.73 and -0.72 respectively, n=16) indicating that χlf is being controlled by the coarse magnetic grains [7]. A significant positive linear correlation exists between χlf and SIRM (r= 0.99, n=16) signify these parameters are chiefly controlled by a common type of magnetic minerals [88]. The χlf and χfd% are negatively correlated (r= -0.62) (Fig. 3) and a positive linear correlation between heavy metals and magnetic minerals in moderate polluted areas. The SIRM reveals a trend be contingent on the χlf and same as χARM and ARM values. The χfd% are of higher values at the bar-mouth except at the B4 station, further confirming the presence of anthropogenic inputs. The Al_2O_3 content shows significant negative correlation with sand (r= -0.88, n=16) and significant enrichment of silt (r= 0.75, n=16) and clay (r= 0.87, n=16) contents, respectively. These parameters confirm the association of these elements in the detrital origin of estuarine sediments [24]. The principal component analysis was employed for the sediments, and results are presented in the Fig. 14a. A varimax rotation was done for the variables, and it formulated three components. The first component accounts for 49.98% of total variance with an eigen value of 10.49. It has high positive loading on silt, $CaCO_3$, clay, Cr, Ni, Pb, SIRM/χlf and χARM/χlf. At the same time, strong negative loading on sand, χlf and SIRM. These parameters indicates the association in the fine sediments. The second component comprises with a positive loading of Zn, Pb, Ti, S-ratio and HM% with an eigen value of 3.85, variance of 18.32% and cumulative percentages of 68.31. This confirms the effluent discharges from the industrial areas and the oil spill from the harbor indicating the presence of anthropogenic and pollution activities. Finally, the third component comprises of positive loading of χlf, ARM, and χARM with an eigen value of 2.34 and variance of 11.14%. The PCA analysis reveals that the elements show significant correlation among each other, which corroborates the results from correlation analysis indicates the influence of grain size in the distribution.

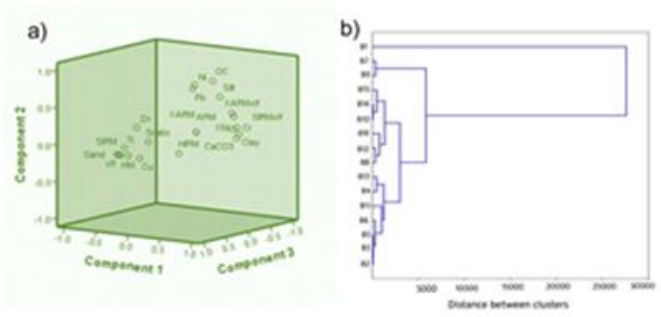

Figure 14. (a) Factor plots depicting the associations between the selected parameters, (b) Hierarchical cluster dendrogram (wards method) exhibits the similarities among the sampling stations in the study area

The cluster analysis were carried out to understand the similarity among the magnetic, geochemical and sedimentological characteristics. The result reveals the

association of 4 cluster (Fig. 14b). The first cluster represents the stations viz., B2, B3, B5, B9, B11, B4 and B13 showing similar affinity of magnetic, trace, heavy metals and grain size composition, specifies the influence of sediment source from the Chaliyar River.

The second cluster (B8, B12, B16, B10, B14 and B15) signifies the characteristic of estuarine nature. The B6 and B7 represent the cluster 3, situated on the north-west side of the Beypore Estuary. They are close to each other and surrounded by mangrove vegetation. In the present study, the trace element shows a varying trend from upper to lower estuary, which may be due to the dredging activities and development of Beypore, fishing harbor (2013 onwards). Moreover, the construction of a breakwater with a length of 1130m and 860m on the south and north side of the Beypore played a crucial role on sediment grain size and trace elements variation from upper to lower estuary. The present study was compared with the previous findings [24], reveals the two-fold enrichment of Cr and Cu, whereas depletion of Pb, Mn, Fe_2O_3, and non-traceable of Co contents.

The dynamic sedimentary environment can be reflected in the relationship between sediment size and magnetic properties. Based on the distribution, correlation coefficient, and factor analysis between the magnetic (χfd%, SIRM, HIRM χARM, χARM/SIRM, χARM /χlf) and grain size parameters for the Beypore Estuary, the result corroborate the enrichment of magnetic parameters in the particular sediment fraction and their distributions are influenced by particle size. Similar results were reported elsewhere [89]. The enhanced chemical weathering and fluvial discharge will increase the χlf, χfd, Cu and Pb contents. These results suggest the presence of enhanced anthropogenic activities in the region. The precipitation increases the weathering, erosion, and transportation of terrigenous materials result in relatively higher accumulations of minerals. The tidal surges control the distributions of metals in the lower parts of the estuary. The correlation between χ and SIRM suggests that the majority of the sediments are dominated by ferrimagnetic minerals, whereas para and diamagnetic minerals have very less influence. The processes of trace metals in the estuarine environment directly influence the various processes associated with the hydrological processes within the transitional estuarine zone. The possible reasons for the enhancement of geochemical and magnetic elements may be the industrial effluents, sludge, and urban wastewater, and the high rate of natural weathering due to the alterations of the land area and rainfall.

III.CONCLUSION

We draw the following conclusions based on the environmental magnetic investigations of the Beypore sediments:

- The magnetic behavior, geochemical affinity and grain size parameters for the Beypore Estuary and their influence on environmental processes are elucidated.
- The magnetic parameters viz., χlf, χfd%, ARM, HIRM, χARM, S-ratio, and SIRM shows a dissimilarity in their distribution from upper to lower estuary.
- The magnetic parameters such as S-ratios, χlf, χARM, SIRM and IRM confirms the presence of ferrimagnetic minerals such as magnetite in the estuary.
- The elemental distribution of major, trace, and REEs exhibits enrichment and depletion, inferring the variation in geochemical affinity throughout the estuary.
- The weathering indices (CIA, A-CN-K plot) attributes intense chemical weathering in the lower estuary, intermediate and weak weathering in the middle and upper estuary. Further, the Beypore

sediments exhibit immaturity (CIA and ICV ratios) with weak to intense chemical weathering.

- The textural analysis reveals the distribution of sediments, from coarse grained to silty clay type from upper to lower estuary indicating different depositional setting.
- The micro-texture of quartz grains attributed that the sediments of the upper estuary are deposited by the mechanical processes. The middle estuary are reflected by mechanical-chemical processes whereas the lower estuary underwent intense chemical weathering and prolonged diagenesis. This further corroborate with the results of geochemical analyses.
- The physical and chemical weathering, industrial and domestic effluents are the primary source of heavy metal assemblages based on metal enrichment (Cr>Zn>Cu>Ni>Pb) in the estuary. In addition, the pollution indices (Igeo, EF and CF) of Cr, Cu and Ni shows moderately contaminated in the estuary.
- Magnetic enhancement, grain size distribution, and heavy metal enrichment in the sediments are attributed to hydrodynamic processes (waves, currents and tides), diagenetic changes, and anthropogenic interface (dredging, and construction of coastal structures).
- The relationship between the magnetic variability, heavy metals, trace elements and the grain size decipher the combination of natural and anthropogenic activities, controlling the environmental processes in the estuary.

IV. ACKNOWLEDGEMENTS

The authors are grateful to the Director, National Centre for Earth Science Studies, Thiruvananthapuram, for providing all the facilities. PBS would like to acknowledge the Kerala State Council for Science Technology and Environment (KSCSTE) for providing financial aid (082/FSHP-ESS/2013/KSCSTE) for this study. PBS would like to express sincere gratitude to Dr. L. Sheela Nair (Group Head MGG) for her unflinching contribution. The authors are thankful to Dr. Reji Srinivas, M K Sreeraj, Dr. Shynu and M. Ajith Kumar for their support during the field work at Calicut. Thanks are due to Jithin Jose and Naveen Kumar, Research scholars, Mangalore University for their help in the magnetic analyses.

V. REFERENCES

[1]. Dionne JC (1963) Towards a more adequate definition of the St. Lawrence estuary. Z. Geomorph., 7, 36-44 (1

[2]. El Wakeel SK, Riley JP (1957) The Determination of Organic Carbon in Marine Mud. Int. J. Mar. Sci. 22, 180–183.

[3]. Narayana AC, Ismaiel M, Priju CP (2021) An environmental magnetic record of heavy metal pollution in Vembanad lagoon, southwest coast of India. Mar Pollut Bull. doi: 10.1016/j.marpolbul.2021.112344.

[4]. Chan LS, Yeung CH, Yim WWS, Or OL (1998) Correlation between magnetic susceptibility and distribution of heavy metals in contaminated sea-floor sediments of Hong Kong Harbour. Environ. Geol. 36, 77–86.

[5]. Zhang W, Lizhong Yu, Hutchinson SM (2001) Diagenesis of magnetic minerals in the intertidal sediments of the Yangze Estuary, China, and its environment significance. Sci Total Environ. 5, 266,166–175.

[6]. Scoullos M, Botsou F, Zeri C (2014) Linking Environmental magnetism to geochemical studies and management of Trace metals. Examples from fluvial, estuarine and marine systems. Minerals 4,716–745.

[7]. Thompson R, and Oldfield F (1986) Environmental Magnetism. Allen & Unwin: Springer, London. , p.227.

[8]. Maher B, Thompson R (1999) Quaternary Climates, Environments and Magnetism, ISBN

0521624177. Cambridge, UK: Cambridge University Press pp.402.

[9]. Oldfield E, Kyung H, Timken C, Montez B, Ramachandran R (1985) High-resolution solid-state NMR of quadrupolar nuclei. Nature, 318,163–165.

[10]. Bityukova L, Scholger R, Birke M (1999) Magnetic susceptibility as indicator of environmental pollution of soils in Tallinn. Phys. Chem. Earth 24, 829–835.

[11]. Venkatachalapathy R, Veerasingam S, Basavaiah N, Ramkumar T, Deenadayalan K (2011a) Environmental magnetic and petroleum hydrocarbons in marine sediment cores from north east coast of Tamil Nadu, Bay of Bengal, India. Mar Poll. Bull. 62, 681–690.

[12]. Venkatachalapathy R, Veerasingam S, Basavaiah N, Ramkumar T, Deenadayalan K (2011b) Environmental magnetic and geochemical characteristics of Chennai coastal sediments, Bay of Bengal, India. J. Earth Syst. Sci. 120, 885–896.

[13]. Prajith A, Rao VP, Chakraborthy P (2015) Distribution, provenance and early diagenesis of major and trace metals in sediment cores from the Mondovi estuary, western India. Estuar. Coast. Shelf Sci., 170; 1-13

[14]. Tyson S, Nath BN, Sangeetha N, Borole, DV, Pierre S, Yazing AK (2017) Offshore sediments record the history of onshore iron ore mining in Goa state, India. Mar. Pollut. Bull., 114, 805–815.

[15]. Lone AM, Hema A, Rayees AS, Sangode SJ (2018) Environmental Magnetism and Heavy metal Assemblages in Lake Bottom sediments, Anchar Lake, Srinagar, and NW Himalaya, India. Int. J. Environ. Sci. 12,489–502.

[16]. Shankar R, Prabhu CN, Warrier AK, Kumar GTV, Sekar B (2006) A multi-decadal rock magnetic record of monsoonal variations during the past 3,700 years from a tropical Indian tank. J. Geol. Soc. India 68, 447¬–459.

[17]. Sandeep K, Shankar R, Warrier AK, Yadava MG, Ramesh R, Jani RA, Weijian Z, Xuefeng L (2017) A multy-proxy lake sediment record of Indian summer monsoon variability during the Holocene in southern India. Palaeogeogr. Palaeoclimatol. Palaeoecol. 476, 1–14.

[18]. Paropkari AL, Topgi RS, Rao ChM, Murty PSN (1980) Distribution of Fe, Mn, Ni, Co, Cu and Zn in nonlithogenous fractions of sediments of Gulf of Kutch I.J. Mar. Sci., 9, 54–55.

[19]. Wang Y, Lam KM, Lu Y (2018) Settling velocity of fine heavy particles in turbulent open channel flow. Phys. Fluids 30:095106.

[20]. Chaparro MAE, Suresh G, Chaparro MAE, Ramasamy V, Sundarrajan M (2017) Magnetic assessment and pollution status of beach sediments from Kerala coast (southwestern India). Mar. Pollut. Bull 117, 171–177.

[21]. James EJ, Sreedharan RE (1983) The exchange of fresh and salt waters in the Beypore estuary on the Malabar Coast. J. Instn. Engrs. (India), 64: Cl 2, 81–87.

[22]. Premchand K, Harish CM, Nair MNM (1987) Hydography of the Beypore estuary, Proc. Natn. Sem. Estuarine Management, Trivandrum. pp. 44–48.

[23]. Anilkumar N, Ravichandran C, Sankaranarayanan VN, Josanto V (1998) Residual fluxes of water, salt and suspended sediments in the Beypore estuary. Indian J. Mar. Sci. 27, 157–162.

[24]. Nair MN, Ramachandran KK (2002) Textural and trace elemental distribution in sediments of the Beypore estuary (SW coast of India) and adjoining inner shelf. Indian J. Mar. Sci, 31, 295–304.

[25]. Anilkumar N, Sankaranarayanan VN, Josanto V (1999) Studies on mixing of the waters of different salinity gradients using Richardsons number and the suspended sediment distribution in the Beypore estuary, southwest coast of India. Indian J. Mar. Sci. 28, 29–34.

[26]. Sreenivasulu G, Praseetha BS, Daud NR, Varghese TI, Prakash TN, Jayaraju N (2019)

Benthic foraminifera as potential ecological proxies for environmental monitoring in coastal regions: A study on the Beypore estuary, Southwest coast of Mar. Pollut. Bull, 138, 341–351. https://doi.org/10.1016/j.marpolbul.2018.11.058.

[27]. Nair MNM (1995) (unpublished Ph.D. thesis). Studies on Beypore Estuary: Trace metals Distribution and physico-chemical characteristics. Thesis submitted to Cochin University of Science and Technology.

[28]. Ambili V (2010) (Unpublished Ph.D. thesis) Evolution of Chaliyar river drainage basin: insight from tectonic geomorphology. Cochin University of Science and Technology, Cochin, Kerala, India.

[29]. Srinivas R, Shynu R, Sreeraj MK, Ramachandran KK (2017) Trace metal pollution assessment in the surface sediments of nearshore area, off Calicut, southwest coast of India. Mar. Pollut. Bull. 120, 370–375.

[30]. Hameed AS, Resmi TR, Suraj S, Warrier UC, Sudheesha M, Deshpande RD (2015) Isotopic characterization and mass balance reveals groundwater recharge pattern in Chaliyar river basin, Kerala, India. J. Hydrol. Reg. Stud. 4, 48–58.

[31]. Nazimuddin, M) (Unpublished Ph.D. thesis). Coastal hydrogeology of Kozhikode, Kerala. Cochin University of Science and Technology, Cochin, Kerala, India.

[32]. CGWB (2009) Groundwater Information Booklet of Kozhikode District, Kerala State. Central Ground Water Board, Ministry of Water Resources, Government of India (CGWB).

[33]. Soman, K (2002) Geology of Kerala. Geological Society of India, Bangalore, 335p.

[34]. Dearing JA (1999) Environmental Magnetism practical guide. Technical Guide No. 6, Quaternary Research Association, London, 35–62.

[35]. Walden J (1999a) Sample collection and preparation. In: Walden, J., Oldfield, F., Smith, J. (Eds.), Environmental magnetism: a practical guide. Technical Guide No. 6, Quaternary Research Association, London, 26–34.

[36]. Walden J (1999b) Remanence measurements. In: Walden, J., Oldfield, F., Smith, J. (Eds.), Environmental magnetism: a practical guide. Technical Guide No. 6, Quaternary Research Association, London, 63–88.

[37]. Oldfield F (1994) Toward the discrimination of fine-grained ferrimagnets by magnetic measurements in lake and near-shore marine sediments. J. Geophys. Res., 99, 9045–9050.

[38]. Chandana KR, Bhushan R, Jull AJT (2017) Evidence of poor Bottom water ventilation during LGM in the Equatorial Indian Ocean. Front. Earth Sci. 5, 84. https://doi.org/10.3389/feart.2017.00084.

[39]. Satyanarayanan M, Balaram V, Sawant SS, Subramanyam KSV, Krishna GV (2014) High Precision Multi element Analysis on Geological samples by HR-ICP-MS. 28th ISMAS-WS, 181–184.

[40]. Carver E (1971) Procedures in sedimentary petrology. Wiley Interscience, New York, 653p.

[41]. Folk RL (1974) Petrology of Sedimentary Rocks. Hemphill Publishing Co., Austin, 170 p.

[42]. Blott SJ, Pye K (2001) GRADISTAT: a grain size distribution and statistics package for the analysis of unconsolidated sediments Earth Surf. Process. Landf. 26, 1237–1248.

[43]. Gibbs RJ (1965) Error due to segregation in quantitative clay mineral X-ray diffraction mounting. Am. Mineral. 50, 741–751.

[44]. Biscaye PE (1965) Mineralogy and sedimentation of recent deep-sea clay in the Atlantic Ocean and adjacent seas and oceans. Bull. Geol. Soc. America 76, 803. https://doi.org/10.1130/0016-7606.

[45]. Rao VP, Rao RB (1995) Provenance and distribution of clay minerals in the sediments of

the western continental shelf and slope of India. Cont. Shelf Res. 15, 1757–1771.

[46]. Krinsley DH, Doornkamp JC (1973) Atlas of Quartz sand grain surface textures. Cambridge Univ. Press.

[47]. Mahaney WC (2002) Atlas of Sand Grain Surface Textures and Applications. Oxford University Press, New York, 237 p.

[48]. Hutchinson and Mcheman (1947) In: Soil and Plant analysis by Piper. The University of Adelaide, Adelaide, 368p.

[49]. Muller G (1969) Index of geo-accumulation in sediments of the Rhine River. Geo. J. 2, 108–118.

[50]. Wedepohl KH (1995)The composition of continental crust. Geochim. Cosmochim. Acta 59, 1217–1232.

[51]. Sreenivasulu G, Jayaraju N, Reddy SRBC, Lakshmanna B, Rajasekhar M, Nirmala K, Lakshmi PT (2018) Assessment of heavy metal pollution from the sediment of Tupilipalem coast, southeast coast of India. Int. J. Sediment Res, 33, 294–302.

[52]. Blounde MK, Duplay J, Quaranta G (2009) Heavy metal contamination of coastal lagoon sediments by anthropogenic activities: the case of Nador (East Morocco). Environ. Geol. 56, 833–843.

[53]. Szefer P, Geldon J, Ahmed Ali, A Paez Osuna, F RuizFernandes, AC, GuerroGaivan SR (1998) Distribution and association of trace metals in soft tissue and byssus of Mytella strigata and other benthal organisms from Mazatlan Harbour, Mangrove lagoon of the northwest coast of Mexico. Environ. Int., 24,359–374.

[54]. Tomlinson DC, Wilson JG, Harris CR, Jeffrey DW (1980) Problems in the assessment of heavy metals in estuaries and the formation pollution index. Helgol. Mar. Res. 33, 566–575.

[55]. Oldfield, F (1991) Environmental magnetism – a personal perspective. Quat. Sci. Rev. 10, 73–85.

[56]. Dearing JA, Bird PM, Dann RJL, Benjamin SF (1997) Secondary ferromagnetic minerals in Welsh soils: a comparison of mineral magnetic detection methods and implications for mineral formation. Geophys. J. Int. 130:727–736.

[57]. Warrier AK, Sebastian JG, Amrutha K, Sali ASY, Mahesh BS, Mohan R (2021) Magnetic properties of surface sediments in Schirmacher Oasis, East Antarctica: spatial distribution and controlling factors. J. Soils sediments 21, 1206–1221.

[58]. Taylor SR, McLennan SM (1985) The continental crust: Its composition and Evolution. Blackwell, Oxford.

[59]. McLennan SM (2001) Relationships between the trace element composition of sedimentary rocks and upper continental crust Geochem. Geophys. Geosyst. 2. https://doi.org/10.1029/2000GC000109

[60]. Anilkumar N, Dineshkumar PK (2002) A study on the seasonal dynamics of Beypore estuary, Kerala coast. Indian Jour. Mar. Sci., 31, 52–58.

[61]. Piper DZ (1974) Rare earth elements in ferromanganese nodules and other marine phases; Geochim. Cosmochim. Acta 38. 1007–1022.

[62]. Pattan JN, Masuzawa T, Borole DV, Parthiban G, Jauhari P, Yamamoto M (2005) Biological productivity, terrigenous influence and noncrustal elements supply to the central Indian Ocean Basin: Paleoceanography during the past 1 Ma. J. Earth Syst. Sci. 114, 63–74.

[63]. Sholkovitz ER (1995) The aquatic chemistry of rare earth elements in rivers and estuaries. Aquatic Geochemistry 1, 1–34.

[64]. López-González N, Borrego J, Carro B, Grande JA, De la Torre ML, Valente T (2012) Rare-earth-element fractionation patterns in estuarine sediments as a consequence of acid mine drainage: A case study in SW Spain. Boletín Geológico y Minero, 123, 55–64, ISSN: 0366-0176.

[65]. Nesbitt HW, Young GM (1982) Early Preterozoic climates and plate motions inferred from major

element chemistry of lutites. Nature, 299, 715–717.

[66]. Bock B, McLennan SM, Hanson GN (1998) Geochemistry and provenance of the Middle Ordovician Austin Glen Member (Normanskill Formation) and the Taconian Orogeny in New England. Sedimentology, 45, 635–655.

[67]. Garcia D, Ravenne C, Maréchal B, Moutte J (2004) Geochemical variability induced by entrainment sorting: quantified signals for provenance analysis. Sediment Geol. 171, 113–128. https://doi.org/10.1016/j.sedgeo.2004.05.013.

[68]. Nesbitt HW, Young GM (1984) Prediction of some weathering trends of plutonic and volcanic rocks based on thermodynamic and kinetic considerations. Geochim Cosmochim Acta. 48, 1523–1534.

[69]. Cox R, Lowe DR, Cullers RL (1995) The influence of sediment recycling and basement composition on evolution of mudrock chemistry in the southwestern United States. Geochim. Cosmochim. Acta. 59, 2919–2940.

[70]. Long X, Yuan C, Sun M, Xiao W, Wang Y, Cai K, Jiang Y (2012) Geochemistry and Nd isotopic composition of the Early Paleozoic flysch sequence in the Chinese Altai, Central Asia: evidence for a northward-derived mafic source and insight into Nd model ages in accretionary orogeny Gondwana Res., 22, 554-566.

[71]. Hayashi KI, Fujisawa H, Holland HD, Ohmoto H (1997) Geochemistry of ~1.9 Ga sedimentary rocks from northeastern Labrador. Canada. Geochim. Cosmochim. Acta.61, 4115–4137.

[72]. Floyd PA, Winchester JA, Park G (1989) Geochemistry and tectonic setting of Lewisian clastic metasediments from the Early Proterozoic Loch Maree Group of Gairloch. NW Scotland. Precambrian Res. 45, 203–214.

[73]. Long X, Sun M, Yuan C, Xiao W, Cai K (2008) Early Paleozoic sedimentary record of the Chinese Altai: Implications for its tectonic evolution. Sedimentary Geol. 208, 88–100.

[74]. Armstrong-Altrin JS (2015) Evaluation of two multidimensional discrimination diagrams from beach and deep-sea sediments from the Gulf of Mexico and their application to Precambrian clastic sedimentary rocks. Inter. Geol. Rev. 57, 1446–1461.

[75]. Roser BP, Korsch RJ (1988) Provenance signatures of sandstone-mudstone suites determined using discrimination function analysis of major-element data. Chem. Geol. 67, 119–139.

[76]. Varghese TI, Prakash TN, Nagendra R, Nagarajan R (2018) Sediment geochemistry of 961 coastal environments, southern Kerala, India: implication for provenance. Arab. J. Geosci. 11, 61. https://doi.org/10.1007/s12517-018-3406-9.

[77]. Elkadya AA, Sweet ST, Wade TL, Klein AG (2015) Distribution and assessment of heavy metal in the aquatic environment of Lake Manzala, Egypt. Ecol. Indic. 58, 445–457.

[78]. Gopal V, Nithya B, Magesh NS, Jayaprakash M (2018) Seasonal variations and environmental risk assessment of trace elements of Uppanar River estuary, southern India. Mar. Pollut. Bull., 129, 347–356.

[79]. Savvides C, Papadopoulos A, Haralambous KJ, Laoizidou M (1995) Sea sediments contaminated with heavy metals: metal speciation and removal. Water Sci. Technol. 32, 65–73.

[80]. Thamban M, Rao VP, Schneider RR (2002) Reconstruction of late Quaternary monsoon oscillations based on clay mineral proxies using sediment cores from the western margin of India. Mar. Geol., 186, 527–539.

[81]. Madhavaraju J, García y Barragán JC, Hussain SM, Mohan SP (2009) Microtextures on quartz grains in the beach sediments of Puerto Peñasco and Bahia Kino, Gulf of California, Sonora, Mexico: Revista Mexicana de Ciencias Geológicas. 26, 367–379.

[82]. Krinsley DH, Donahue J (I968) Environmental interpretation of sand grain surface textures by electron microscopy. Geol. Soc. Am. Bull. 79: 743–748.

[83]. Armstrong-Altrin JS, Natalhy-Pineda O (2014) Macrotextures of detrital sand grains from the Tecolutla, Nautla, and Veracruz beaches, western Gulf of Mexico, Mexico: implications for depositional environment and paleoclimate. Arab. J. Geosci. 7, 4321–4333.

[84]. Tiju VI, Prakash TN, Sheela Nair L, Sreenivasulu G, Nagendra R (2021) Reconstruction of the paleoenvironment of the late Quaternary sediments of the Kerala coast, SW India. Journal of Asian Earth Sciences 222, https://doi.org/10.1016/j.jseaes.2021.104952.

[85]. Krinsley DH, Mccoy FW (1977) Significance and origin of surface textures on broken sand grains in deep-sea sediments. Sedimentology 24 (6), 857–862.

[86]. Setlow LW, Karpovich RP (1972) “Glacial” micro-textures on quartz and heavy mineral sand grains from the littoral environment. J. Sediment. Res. 42, 864–875.

[87]. Avinash K, Kurian JP, Warrier AK, Shankar R, Vineesh TC (2016) Sedimentary sources and processes in the eastern Arabian Sea: Insights from environmental magnetism, geochemistry and clay mineralogy. Geosci. Front. 7, 253–264.

[88]. Ouyang T, Mingkun Li, Erwin A, Shuqing F, Guodong Jia, Wei, L (2017) Magnetic properties of surface sediments from the Pearl River Estuary and its adjacent waters: Implication for provenance. Mar. Geol. 390, 80–88.

[89]. Chu N, Yang Q, Liu F, Luo X, Cai H, Yuan L, Huang J, Li J (2020) Distribution of magnetic properties of surface sediment and its implications on sediment provenance and transport in Pearl River Estuary. Mar. Geol. 424, https://doi.org/10.1016/j.margeo.2020.106162.

Cite this article as :

B. S. Praseetha, V. I. Tiju, T. N. Prakash, G. Sreenivasulu, R. Nagendra, "Environmental Magnetism, Geochemical and Textural Characteristics of the Sediments of Beypore Estuary, Northern Kerala, India : Implication on Environmental Processes", International Journal of Scientific Research in Science and Technology (IJSRST), Online ISSN : 2395-602X, Print ISSN : 2395-6011, Volume 9 Issue 3, pp. 314-334, May-June 2022. Available at doi : https://doi.org/10.32628/IJSRST229367
Journal URL : https://ijsrst.com/IJSRST229367